Spatiotemporal assessment of extreme heat risk for high-density cities: A case study of Hong Kong from 2006 to 2016

Authors: Junyi Hua[1], Xuyi Zhang[1], Chao Ren[1,*], Yuan Shi[2], Tsz-Cheung Lee[3]

1. Faculty of Architecture, The University of Hong Kong, Pokfulam, Hong Kong, China

2. Institute of Future Cities, The Chinese University of Hong Kong, Shatin, Hong Kong, China

3. Hong Kong Observatory, Kowloon, Hong Kong, China

E-mail addresses:

Junyi Hua: jhua@hku.hk

Xuyi Zhang: zhang_xuyi@foxmail.com

Chao Ren: renchao@hku.hk

Yuan Shi: shiyuan@cuhk.edu.hk

Tsz-Cheung Lee: tclee@hko.gov.hk

*Corresponding author:

Dr. Chao Ren

E-mail address: renchao@hku.hk

Postal address: 4/F, Knowles Building, Faculty of Architecture, The University of Hong Kong, Pokfulam, Hong Kong, China

Highlights

- Heat hazard, population exposure, and demo-socioeconomic vulnerability were integrated.
- The heat risk patterns varied between daytime and nighttime.
- High heat risk in core urban areas and increasing heat risk in some new towns.
- The underlying determinants of high heat risks were analyzed and discussed.
- The heat risk maps inform local heat-health actions and healthy urban planning.

Spatiotemporal assessment of extreme heat risk for high-density cities: A case study of Hong Kong from 2006 to 2016

Abstract

High-density cities are faced with growing extreme hot weather driven by climate change and local urbanization, but localized heat risk detection is still at an early stage for most cities (Watts et al., 2019). This study developed a spatiotemporal hazard-exposure-vulnerability assessment of the extreme heat risk in Hong Kong for 2006, 2011, and 2016 integrating cumulative very hot day hours and hot night hours in summer, population density and a principal component analysis (PCA) of demo-socioeconomic characteristics. The risk was found spatially variant, and high-risk spots were identified at the community scale for both daytime and nighttime with underlying determinants behind. In both the daytime and the nighttime, high risk mainly occurred in the core urban areas. Nearly 10 more hot-spots were found in the nighttime than those in the daytime. Several old communities in Kowloon stayed at high risk from 2006 to 2016. Some new towns in the New Territories turned to be at higher risk in 2016 compared to 2006 and 2011, and this result showed signs to be emerging hot-spots in the near future. This study would be a useful reference for community-scale heat risk assessment and mitigation for the development of healthy and sustainable high-density cities.

Keywords:

Extreme hot weather; Heat vulnerability; Heat risk; Spatial assessment; High-density cities; Hong Kong

1. Introduction

1.1 The need of a spatiotemporal assessment of extreme heat risk for high-density cities

Frequent, prolonged and intensified heatwaves as a consequence of climate change, have turned to be an increasing threat to human health (Luber & McGeehin, 2008; Mora et al., 2017). Climate change boosts the occurrence of extremely high temperatures concerning the frequency, intensity, and duration and hence increases the heat-related morbidity and mortality worldwide (Guo et al., 2018), especially in urban areas accommodating more than half of the global population (IPCC, 2014). High-density cities are at higher risks due to dense population of higher exposure and vulnerability and the urban heat island (UHI) effect aggravating extreme heat (Li & Bou-Zeid, 2013). Hundreds of cases of heat caused excess human mortality have been recorded over the globe (Åström et al., 2011; Li et al., 2016; Mora et al., 2017), and the adverse health impacts of extreme heat events have been widely evaluated in different countries and cities (Basu, 2009; Gasparrini et al., 2015). Tropical and sub-tropical countries and regions will witness the most heatwave-related excess mortality without adaptation (Guo et al., 2018). Therefore, more emphasis should be placed on high-density cities in the regions. It is of vital importance to locate the groups of city dwellers with higher social vulnerability to the impacts of the extreme heat events within cities (Johnson et al., 2012). The vulnerability to extreme heat has been found associated with demographic and socioeconomic status (Chan et al., 2012; Gronlund et al., 2015; Uejio et al., 2011), which creates some more vulnerable groups featured with the elderly, social isolation, and low socioeconomic status. The aging populations in some regions of the world, like East Asia, raise the vulnerability due to the elderly's low capacity of resistance to heatwaves (Åström et al., 2011; Li et al., 2016). The varying demographic and socioeconomic status could make the heat vulnerability unevenly distributed and change with time (Cutter & Finch, 2008). The increasingly severe extreme heat conditions (Sun et al., 2014) in high-density cities with great spatiotemporal variability (Shi et al., 2019) could also accentuate the heat risk of the more vulnerable population segments. However, localized heat risk detection is still at an early stage for most cities (Watts et al., 2019). Recent studies on heat risk assessment have been mainly carried out for low- to medium density cities in Europe and North America with temperate climates (Bradford et al., 2015; Ho et al., 2018; Morabito et al., 2015; Tomlinson et al., 2011), but a special emphasis on extreme heat risk for high-density cities in subtropical regions is awaited. Moreover, while most of the previous studies on heat risk inclined to focus on the very hot weather in the daytime, the high temperature at night (hot night) which is partly attributed to the compact built environment and may have significant health impacts (Ho et al., 2017; Wang et al., 2019) has not been fully investigated. To sum up, for preserving sustainable urban habitat, an integrated spatiotemporal assessment providing the dynamic information about the daytime and nighttime extreme heat risk for high-density cities is imperative for mitigating the adverse impacts from the heat hazard in targeted zones or communities in advance instead of remedying the damage with hindsight. In this study, Hong Kong is taken as an exemplary case in view of the increasing occurrence of extreme heat events during both the daytime and nighttime in summer in the context of global climate change and local urbanization, the complex urban setting and hilly morphology, the high-density population, and the increasing vulnerable sub-groups of the elderly and poor socioeconomic status (see Section 2.1).

1.2 Theoretical and methodological issues of heat risk mapping and assessment

Based on the Crichton's Risk Triangle framework and the Intergovernmental Panel on Climate Change's (IPCC) conception, a risk is defined as a function of three components, namely hazard, exposure, and vulnerability (Crichton, 1999; IPCC, 2014), which are, specifically, the frequency and intensity of hazards, the presence of assets exposed, and the propensity or predisposition to be adversely affected. Anyone of the three elements is indispensable if a risk exits. The integrated risk to map is, therefore, the overlay of three layers separately estimated. The conceptual framework could help inspire ways to manage risk from the perspectives of the key components. The framework has been increasingly utilized in risk assessment studies, for example, in the fields of flood risk (Kaźmierczak & Cavan, 2011) and heat risk in urban contexts (Chen et al., 2018; Dong et al., 2014; Ho et al., 2015; Morabito et al., 2015; Verdonck et al., 2019; W. Zhang et al., 2019).

Mapping spatial distributions of heat risk is a major subject in the literature of heat risk assessment and benefits decision-making (Wolf et al., 2015), the very first step of which is to map the spatial patterns of the extreme hot weather conditions. A common approach is using remote sensing data like Moderate Resolution Imagining Spectroradiometer (MODIS) to estimate land surface temperature (Chen et al., 2018; Morabito et al., 2015). Data derived from meteorological stations are long-track sources of air temperature and have also been utilized to depict extreme hot weather conditions (Aubrecht & Ozceylan, 2013; Gronlund et al., 2015), but what is often used is daily mean or maximum temperature. Obviously, hourly recorded data could help more precisely simulate extreme hot weather conditions separately in the daytime and nighttime within a day, which has been rarely employed. Shi et al. (2019) used station-measured hourly air temperature to evaluate the spatial variability of the extreme hot weather conditions in Hong Kong with the method of land use regression. Hence, the approach was adopted and adjusted to the present study at the community level for a spatiotemporal illustration of the growing extreme heat in both the daytime and nighttime in a high-density city.

The vulnerability of population or a specific population group, for example, the elderly (Morabito et al., 2015) to extreme heat, is another element to measure for heat risk assessment.

The factor analytical approach has been widely applied to embrace multiple factors for measuring heat vulnerability (Bao et al., 2015; Bradford et al., 2015; Johnson et al., 2012; Nayak et al., 2018; Wolf & McGregor, 2013). It could benefit both scientific research and practical decision-making by unifying multiple determinants and presenting visual results. Among the drivers influencing the population's heat vulnerability, demographic and socioeconomic characteristics represent a dominant aspect from the individual perspective probably impacting people's adaptive capacity to get over heat hazards, which concerns financial capabilities, physical wellness, emotional conditions, awareness of risk mitigation, living environment, healthcare access, etc. (Rohat et al., 2019). Romero-Lankao et al. (2012) summarized the influence of some factors on the vulnerability to the temperature-related hazards in a meta-analysis, including air-conditioning, education, income, poverty, housing quality, social isolation, healthcare access, age, etc., and found expected influences in some of the factors. Gronlund (2014) made a deep review of the similar socioeconomic determinants of the vulnerability to the heat-related health effects. The elderly and ones who live alone have been found with a higher chance of suffering from heat-related problems. Previous studies have proved that older populations are vulnerable groups to heat exposure because aging will deteriorate people's adaptation to extreme heat events and recovery capacity from heat stroke (Åström et al., 2011; Kenny et al., 2010). The high probabilities of having chronic diseases and living alone also exacerbate their vulnerability towards extreme heat events (Bao et al., 2015; Victor et al., 2000). The association between living alone status and higher mortality and morbidity risks has also been proved (Klinenberg, 2003; Semenza et al., 1996). A study in Hong Kong found people living alone were more sensitive to high-temperature effects on help-seeking behavior (Chan et al., 2011). Low education attainment may increase heat vulnerability as it is likely to be associated with a lack of related knowledge on heat risk and awareness of risk mitigation (Ho et al., 2018; Johnson et al., 2012). Chan et al. (2012) also identified people living in low socioeconomic status were more vulnerable to heat-related mortality in Hong Kong. Gronlund (2014) points out that income may play as a mediator between the heat effects and people's living conditions that are closely related to the dwellers' vulnerability to heat waves (Loughnan et al., 2015; Santamouris & Kolokotsa, 2015). The influence of demographic and socioeconomic factors on the population's vulnerability to extreme heat has been identified to be with significant spatial variability in many cities (Aminipouri et al., 2016; Bradford et al., 2015; Macnee & Tokai, 2016; Reid et al., 2009; Rosenthal et al., 2014). Furthermore, the heat vulnerability's temporal variation with regard to demographic and socioeconomic factors, which may be intertwined with the spatial variation, also needs attention as the factors are always varying with time under the circumstances of, for example, aging society, widening income gap, urbanization, and migration (Cutter & Finch, 2008).

1.3 Research objectives

Given the currently unknown spatiotemporal variability of the environmentally and demo-socioeconomically determined integrated risk of extreme heat in high-density cities, this paper aims to carry out a holistic spatiotemporal risk assessment based on the Risk Triangle framework for a comprehensive understanding of the extreme heat risk in the high-density city of Hong Kong, which would be useful for the development of heat risk mitigation measures in Hong Kong and future urban planning (Aflaki et al., 2017; Bakhsh et al., 2018). The present study objectives are (1) to develop a localized integrated extreme heat risk index for high-density cities combining the distributions of extreme hot weather conditions, population exposure, and population's heat vulnerability from the demo-socioeconomic perspectives, (2) to map the spatial patterns and temporal trends of the daytime and nighttime extreme heat risks in Hong Kong at the community level in three reference years over a ten-year period between

2006 and 2016, and (3) to identify hot spots of extreme heat risk in Hong Kong and their latent contributors.

2. Materials and methods

2.1 Study area

The study area encompasses the whole territory of the Hong Kong Special Administrative Region of the People's Republic of China (Figure 1). Hong Kong, situated at the eastern side of the mouth of the Pearl River Delta in South China, has a subtropical climate. The local climate is characterized by a hot and humid summer from June to August with a daily mean temperature over 28°C (HKO, 2020b). Against the background of climate change and local urbanization, there is a long-term increasing trend in average temperature and the annual number of hot days (daily maximum temperature of 33°C or above at the Hong Kong Observatory (HKO)) and hot nights (daily minimum temperature of 28°C or above at HKO), resulting an increasing heat health risk to the public. Extreme heat has been getting more frequent and intensive in recent decades in Eastern China (Sun et al., 2014), and Hong Kong has also experienced scorching summer in recent years (Wang et al., 2016), including the record-breaking high temperature events in May 2018 and July 2020 (HKO, 2020c; Wang et al., 2016). Previous studies also suggested that high ambient temperatures and prolonged heat events could have public health impacts in Hong Kong, including increases in hospitalization and mortality risks (Liu et al., 2020).

The city is characterized by high-density built environment and population and extremely high-degree urbanization. The city accommodates over seven million residents within the area of approximately 1106 km^2, of which only 24% is built-up land and 7% is for residential purposes (PlanD, 2019). It causes a high population density, about 6777 people/km^2 in metro areas on average. The large population of Hong Kong is mainly distributed in urban areas that consist of two parts, the core urban areas (Kowloon and the northern part of Hong Kong Island) and the new towns in the New Territories. Moreover, the population density varies spatially. The unbalanced population density is bound to an unbalanced exposure to the extreme hot weather conditions. Due to the limited built-up land and the large population, the median per capita floor area of accommodation of domestic households was only about 161 square feet in 2016, lower than the figures for other high-density cities in Asia, like Tokyo and Singapore. The dense and narrow dwellings produce poor and tight living conditions and are more likely to cause heat-related health problems (Dunn, 2000). In addition, the city's special geographical and urban characteristics exacerbate the spatial complexity of extreme heat conditions (Shi et al., 2019). The compact urban form embracing high-rise and dense buildings and the mountainous morphology reduce air movements and hence help keep the high temperature in hot summers under the urban heat effect (Peng et al., 2018; P. P.-Y. Wong et al., 2016).

The aging population and the socioeconomic disparity make the city more vulnerable to extreme heat. According to the Hong Kong Population Projection 2017-2066 (CenStatD, 2017e), the current aging trend is expected to continue in the coming decades. The proportion of the residents aged 65 and over is predicted to rise from 16.6% in 2016 to 31.1% in 2036. The positive relationship between hot weather conditions and morbidity/mortality is more significant in elderly population that is more vulnerable to high temperatures due to low adaptive capacity, pre-existing illnesses, social isolation, insufficient air conditioning, and lack of knowledge on and awareness of self-protection (Chau et al., 2009). Hong Kong that ranked the 7th highest Human Development Index (0.933 in 2017) is experiencing an expanding socioeconomic disparity (Wu, 2009). The Gini coefficient, a well-known income inequality index, reached 0.539 in 2016, the highest through 40 years in Hong Kong (CenStatD, 2017c). The ratio of the income of the richest decile to that of the poorest decile increased from 34 in 2006 to 44 in 2016. Based on the 2018 Hong Kong Poverty Situation Report (CenStatD, 2019b), over 1.4 million residents (20.4%) were living under the poverty line before policy intervention. What's worse is that the proportion in elders aged 65 and above was up to 30.9%. The disparity of the demographic and socioeconomic characteristics may link with the variation of the population's heat vulnerability. Its association with temperature-related mortality in Hong Kong has been recognized (Chan et al., 2012). The inequality of the UHI has been found correlated with the unevenly spatially distributed socioeconomic characteristics in Hong Kong (M. S. Wong et al., 2016). A vulnerability index embracing various socioeconomic characteristics could provide a multidimensional construction to identify groups of higher vulnerability (Otto et al., 2017).

2.2 Heat risk mapping and assessment modelling

We referred to the Crichton's conceptual definition of risk triangle (Crichton, 1999) to develop the Hong Kong heat risk maps. Following this concept, the heat risk that is the probability of a loss caused by the hazard (i.e. extreme heat events) in this study, depends on and derives from the combination of the severity, frequency, and duration of the hazard, the exposure of the related population to the hazard, and the vulnerability of the exposed population to the hazard. Therefore, heat risk maps in this study are the integrated results of the layers of hazard, exposure, and vulnerability. The risk triangle offers a concise structure of risk into three separate dimensions to simplify its understanding and enable analysis with GIS (Tomlinson et al., 2011). We adopted consistent methods to develop risk maps for the years 2006, 2011 and 2016, in which census data were released by the Census and Statistics Department, thus it's possible to see the temporal variation based on data in the three reference years during this ten-year period. All the hazard, exposure, and vulnerability layers were calculated at the Large Tertiary Planning Unit (LTPU) level. The whole territory of the city is divided into Tertiary Planning Units (TPUs) by the Planning Department of the HKSAR Government for urban planning purposes. TPUs with small were merged with adjacent TPU(s) to form LTPUs. For each study year, there were about 150 LPTUs with available census data on demo-socioeconomic characteristics. The LTPU is some reflective of the way people live in Hong Kong. The boundary is delineated with the nature of geographic features in the area like roads, railway lines, coastlines, contours, waterways, lot boundaries, and zoning boundaries (PlanD, 2004). The planning purposes make the units reflective of residents' lives and roughly represent communities (Cerin et al., 2016). The availability of the TPU boundaries and the census data allowed the mapping of the hazard, exposure, vulnerability, and the overlaid risk at the community level, especially the establishment of the heat vulnerability index based on the demographic and socioeconomic characteristics for the heat vulnerability maps. The methodological details of the three elements are demonstrated in Subsections 2.3-2.5.

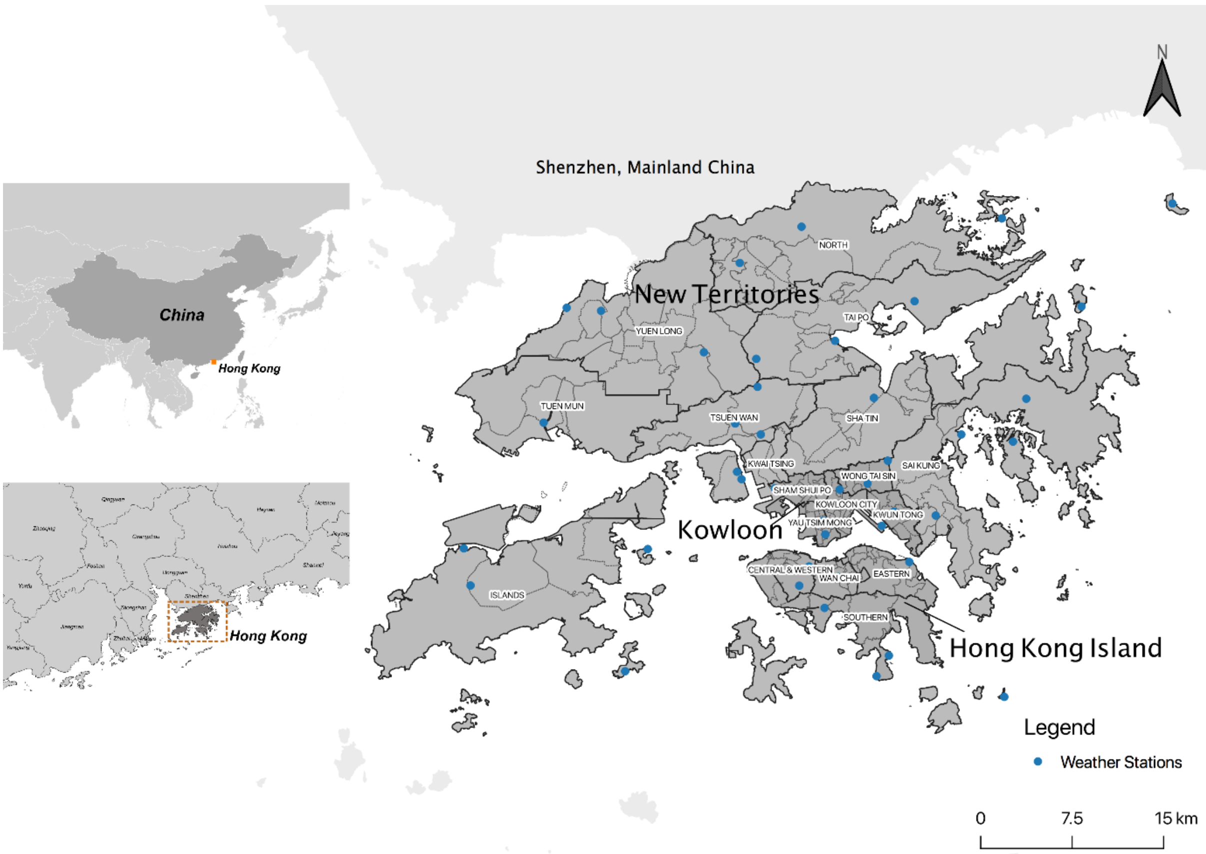

Figure 1. The study area and the location of the weather stations of the Hong Kong Observatory

A heat risk map is the integrated result of heat hazard (spatial distribution of extreme heat events), heat exposure (population distribution), and heat vulnerability (vulnerable groups). Figure 2 presents the workflow of this study. According to previous literature, there has been no unanimous suggestion on weight assignment across the indices under the risk triangle framework (Chen et al., 2018; Ho et al., 2015; W. Zhang et al., 2019). In this study, equal weights were adopted to the layers of the standardized hazard, exposure, and vulnerability values (transformed to z-scores) for the production of a heat risk index that was utilized to generate a heat risk map for each study year, as we attached similar importance to the three facets under the current Hong Kong background. Layer overlaying was conducted in ArcGIS 10.6 software from Environmental Systems Research Institute (ESRI) to produce final risk maps. The unitless risk index that is comparable across LTPUs, as a relative value, was classified into 5 risk categories based on standard deviations (SD) (Cutter & Finch, 2008; Reid et al., 2009) to spatially illustrate risk magnitude:

1. Low: > 1.5 standard deviation (SD) below the mean,
2. Moderately low: 0.5–1.5 SD below the mean,
3. Moderate: 0.5 SD around the mean,
4. Moderately high: 0.5–1.5 SD above the mean,
5. High: > 1.5 SD above the mean.

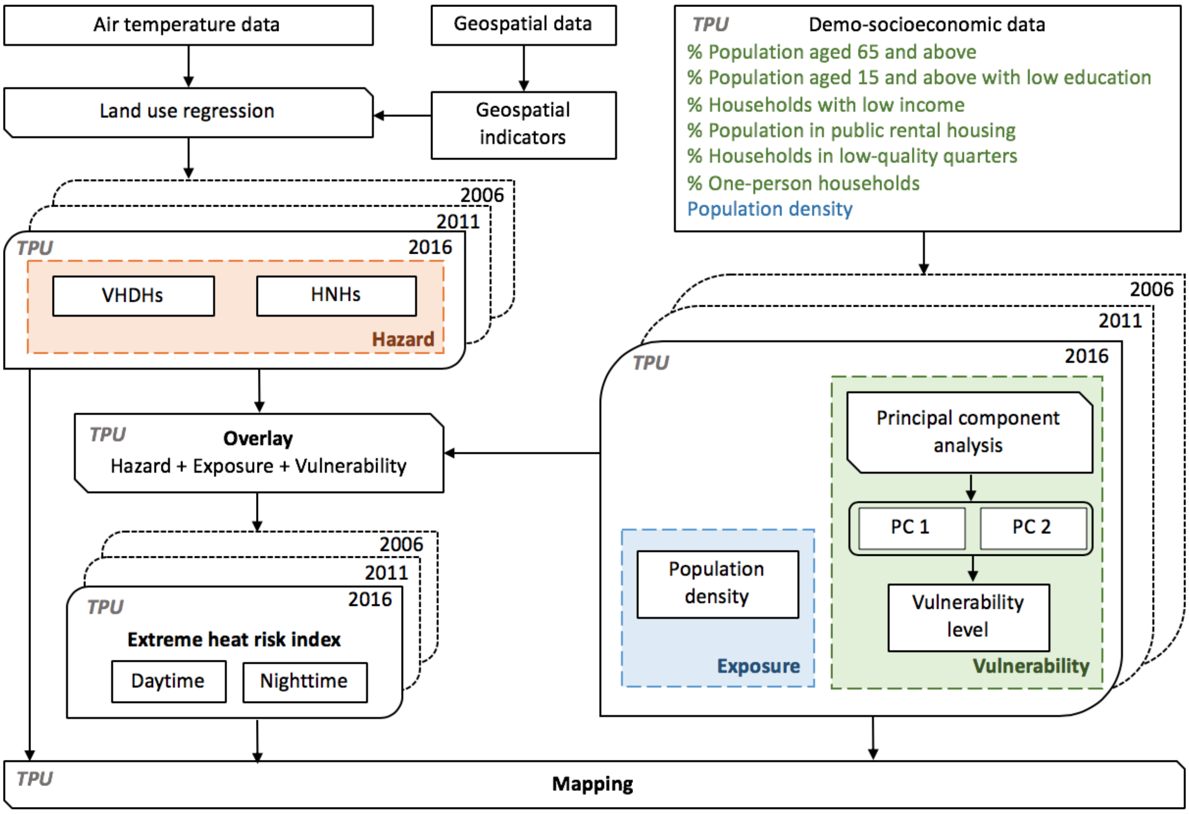

Figure 2. Workflow of the heat risk mapping

2.2.1 Heat hazard

Given the complex urban geographic context of Hong Kong, the extreme hot weather conditions vary spatially due to the heterogeneous land surface features, which have been evidenced by (Shi et al., 2019). The method used by (Shi et al., 2019) is derived and improved from the conventional "land use regression" (Hoek et al., 2008). Compared with the conventional method, the improved method not solely utilizes land-use type, but also incorporates urban surface aerodynamic properties, building morphological factors, weather data from monitoring network, and upper-air sounding data as predictor variables. Therefore, the improved method enables the inclusion of the underlying influence of horizontal advection effect and the interaction between the atmospheric environment and ground surface in the modelling process. We followed Shi et al.'s improved land use regression methods and adjusted at the LTPU scale of the mapping of the extreme hot weather conditions for the years 2006, 2011, and 2016 specifically for the present study. Very hot days and hot nights are widely-used indicators of Hong Kong's extreme hot weather conditions (Lee et al., 2015). Moreover, nighttime extreme heat events may cause a more significant health impact (Ho et al., 2017; Wang et al., 2019). To measure the duration and intensity of such extreme hot weather condition, for each study year (2006, 2011 and 2016), the average annual cumulative very hot day hours (VHDHs, the total number of hours ≥ 33°C in the daytime 7:00 - 18:00 HKT) and hot night hours (HNHs, the total number of hours ≥ 28°C in the nighttime 1:00 - 6:00 and 19:00 - 24:00 HKT) were calculated for summer from June to August according to the hourly air temperature records monitored by a total of forty weather stations of the Hong Kong Observatory (HKO) (Figure 1) for ±2 years of the reference year (2004 - 2008, 2009 - 2013, 2014 - 2018, respectively). The two outcome variables, VHDHs and HNHs, for each study year, were separately mapped in land use regressions with the spatial predictors including land use information, urban road network, spatial distribution of population, natural topography and landscapes, as well as urban land surface morphology in the geographic information system. The description of the predictors is well presented in the paper of Shi et al. (2009). Predictor variables were generated based on the ten buffer widths (100m, 200m, 300m, 400m, 500m, 750m, 1000m, 1500m, 2000m, and 3000m) around the weather stations except for the geo-location and distance-based predictors. A stepwise multiple linear regression with A Distance Decay Regression Selection Strategy (ADDRESS) for a sensitivity test for the buffer predictors was utilized to screen the predictors and optimize the models. The spatial mapping was performed with a resolution of 10m and aggregated at the LTPU level. The land use regression technique helped estimate the extreme hot weather conditions depicted by VHDHs and HNHs on the whole territory of Hong Kong at the TPU scale depending on the powerful predictors. These mapping results are able to illustrate the spatiotemporal variation of Hong Kong's extreme hot weather conditions.

2.2.2 Heat exposure

As every resident is potentially exposed to the heat hazard, we calculated the population density as a proxy to measure heat exposure for each LTPU for the years 2006, 2011 and 2016, separately. Population density has been often used as a proxy to quantify the exposure to hazard in the risk assessment studies (Estoque et al., 2020; Hu et al., 2017; Tomlinson et al., 2011; Verdonck et al., 2019). Open data at the LTPU scale was obtained from the Census and Statistics Department (CenStatD), which provides a more accurate way than other media like nighttime light data to estimate population density (Chen et al., 2018).

2.2.3 Heat vulnerability

Heat vulnerability has been found significantly dependent on and varying with demographic and socioeconomic status (Chen et al., 2018; Gronlund et al., 2015; Johnson et al., 2012; Mushore et al., 2017; Uejio et al., 2011). Some demographic and socioeconomic characteristics are more likely to link with the inability to withstand extreme hot weather. We identified six heat-vulnerability-related indicator variables based on the literature review and the availability of Hong Kong census data and extracted the data from the 2006/2011/2016 Census at the LTPU level for this community-level study. (1) Percentage of population aged 65 and above. The figure for Hong Kong increased from 12.4 in 2006 to 15.9 in 2016 (CenStatD, 2017a), indicating an expanding, large group of high vulnerability. (2) Percentage of population aged 15 and above with low education level. Based on CenStatD's classification on education attainment (highest level attended instead of completed), we defined the low education group as the population with no schooling, pre-primary or primary education attainment. While the percentage notably decreased from 25.4 in 2006 to 20 in 2016, it is still non-negligible. (3) Percentage of one-person households. We used the percentage of one-person households as a proxy for living alone status and social isolation. The Hong Kong census data show high proportions of one-person households increasing from 16.5% in 2006 to 18.3% in 2016. Moreover, people who live alone are more vulnerable to extreme heat events. In domestic one-person households, the proportions of one-elderly-person (aged 65 and above) households rose from 26.9% in 2006 to 33.2% in 2016. (4) Percentage of households with low income. We defined low-income households as ones with monthly household income below the poverty line of the year. The threshold designators were time-variant as proposed by Cutter and Finch (2008) and therefore determined based on the Hong Kong poverty lines for three-person households in 2006, 2011, and 2016 as the average household sizes were 3.0, 2.9, and 2.8, separately. Since the official poverty line was initiated in 2009, we derived HKD10,500 and HKD15,000 for 2011 and 2016. The poverty line for 2006 was calculated in the light of its definition as 50% of the pre-intervention median monthly household income to be HKD 8,750. Limited to the categorization of the monthly household income levels, the thresholds were set to be HKD8,000, HKD10,000, and HKD15,000 for the respective years. (5) Percentage of population living in public rental housing (PRH). The population living in public rental housing (PRH) usually consists of a higher proportion of relatively low-income, elderly, and disabled groups who rent the units with certain discounts from the Hong Kong Housing Authority. The requirements on maximum monthly income and total assets vary with household size. It represents a typical living condition in Hong Kong, accommodating approximately 30% of the total population (CenStatD, 2017a). A substantial duration of overheating in PRH in Hong Kong's summer has been observed (Kwok et al., 2017). (6) Percentage of households living in low-quality quarters. We defined low-quality quarters as both quarters in non-residential buildings, including all units of accommodation in non-residential buildings (such as commercial buildings and industrial buildings), and temporary quarters, including quarters in temporary housing areas as well as private temporary structures such as roof-top structures and contractor's matsheds, places not intended for a residential purpose (such as landings, staircases, corridors, etc.), and vessels (CenStatD, 2019a). These types of households account for over 1 percent in all households in Hong Kong, who bear worse living conditions than ones in PRH.

As the demographic and socioeconomic factors may be correlated, we adopted an inductive method, initially used by (Cutter et al., 2003) for a vulnerability index development, to establish the heat vulnerability index in Hong Kong synthesizing multiple factors. Principal component analysis (PCA) is a widely-used tool in the heat index literature (Bao et al., 2015; Nayak et al., 2018; W. Zhang et al., 2019) to reduce the number of indicators and create independent principal components to reflect the most variance in the original indicators, which, in this study, were six vulnerability-related demographic and socioeconomic variables. IBM SPSS Statistics 26 (IBM Corp, 2019) was applied for the PCA calculation. Kaiser-Meyer-Olkin and Bartlett's tests were executed to examine the data's suitability for the PCA in the light of common variance proportion and identity correlation matrix. Principal components (PCs) with eigenvalues greater than 1 were retained following the K1 rule (Kaiser, 1960). A varimax rotation was then performed to derive orthogonal factors in order to improve the interpretation and dispersion of principal components' loadings. Regression factor scores were then computed for each LTPU in the combination of indicator variables' values and corresponding coefficients. We calculated the integrated vulnerability index score as the sum of the products of each factor score weighted by the corresponding variance explained by the PC. The vulnerability scores were further classified at a five-level scale in the way for the risk index from low to high.

Table 1. Descriptive statistics of the LTPUs

	Min.	Max.	Median	Mean	Std. Dev.	HK Mean
2006						
% Population aged 65 and above	0.033	0.266	0.132	0.130	0.048	0.124
% Population aged 15 and above with low education	0.042	0.431	0.243	0.238	0.091	0.254
% Households with low income	0.013	0.406	0.205	0.203	0.080	0.213

% Population in PRH	0	0.999	0.084	0.213	0.259	0.311
% Households in low-quality quarters	0	0.368	0.005	0.022	0.049	0.013
% One-person households	0.050	0.402	0.169	0.180	0.066	0.165
Population Density	0.137	166.674	28.257	38.360	36.798	6.352
2011						
% Population aged 65 and above	0.035	0.258	0.141	0.136	0.044	0.133
% Population aged 15 and above with low education	0.035	0.363	0.215	0.207	0.079	0.228
% Households with low income	0.018	0.470	0.227	0.218	0.089	0.238
% Population in PRH	0	0.995	0.042	0.197	0.250	0.303
% Households in low-quality quarters	0	0.329	0.006	0.022	0.046	0.014
% One-person households	0.063	0.467	0.165	0.179	0.064	0.171
Population Density	0.145	155.978	27.425	38.522	37.239	6.544
2016						
% Population aged 65 and above	0.085	0.264	0.158	0.159	0.036	0.159
% Population aged 15 and above with low education	0.042	0.358	0.185	0.182	0.072	0.200
% Households with low income	0.076	0.530	0.307	0.289	0.097	0.313
% Population in PRH	0	1.000	0.047	0.201	0.260	0.302
% Households in low-quality quarters	0	0.351	0.007	0.024	0.045	0.016
% One-person households	0.045	0.393	0.172	0.188	0.065	0.183
Population Density	0.154	168.668	26.681	39.140	38.865	6.777

3. Results

3.1 Descriptive statistics of the LTPUs

LTPUs, as the basic units in the study to represent communities in Hong Kong, spatially vary in the geographical, demographic, and socioeconomic features to great extents. The descriptive statistics of the characteristics are presented in Table 1. The percentage of the population aged 65 and above, for example in 2011, ranged from 3.5 to 25.8 with a mean of 13.6 ($\pm$4.4). The proportions of households in PRH, households in low-quality quarters, and one-person households were relatively stable over time from 2006 to 2016. About half of the LTPUs had no PRH, whilst a few in Kowloon and Kwai Chung (LTPU-327) were almost full of PRH, which is highly associated with the LTPU delineation. Most of the LTPUs with high percentages of households living in low-quality quarters (over 10%) were clustered in the northern part of the New Territory, adjoining the city of Shenzhen, Mainland China, except a very special one in the south of Kowloon covering Hung Hom (LTPU-213-217), which ranked top at 35% and simultaneously reached a high ratio of one-person households at 36%. Besides, LTPUs with the highest proportions of one-person households (over 30%) were mainly scattered around Central, the central business district of Hong Kong. The other features at the LTPU level including population density and the percentages of the elderly, ones with low education attainment, and households with low income presented rising trends in the ten years.

3.2 Heat hazard

Figure 3 jointly shows the spatial-temporal patterns of VHDHs and HNHs at the LTPU level. There is an increase in the extreme hot weather conditions from 2006 to 2016 in both the daytime and nighttime. Strong intra-city variability of the extreme hot weather conditions enhanced by the UHI effect could be easily observed. During the daytime, densely built-up areas with high-rise buildings exacerbated the high temperatures, and during the nighttime, these areas kept to be the hotspots. Fig 3 also illustrates that there is a noticeable increase in the VHDHs and HNHs in Hong Kong in the decade. This is generally in line with observed the long-term increasing trend of annual number of very hot days and hot nights (HKO, 2020a). The mean value of the average annual cumulative VHDHs across LTPUs rose from 54 (±22) hours in 2006 to 93 (±32) hours in 2011 then to 110 (±33) hours in 2016 and that of HNHs increase from 376 (±169) hours in 2006 to 425 (±211) hours in 2011 then to 493 (±213) hours in 2016. The significant temporal differences across years were testified with the one-way ANOVA results ($F(2, 451) = 143.25\ and\ 13.11, p < 0.001$). In detail, Kowloon, the northern part of Hong Kong Island, and Tsuen Wan (TW) new town have become the main hotspots in both the daytime and nighttime since 2011, though in 2006, only sporadic patches in these areas greatly suffered from VHDHs. However, the HNHs in these areas kept at relatively high levels over 400 hours between 2006 and 2016. For newly developed areas, a large area in the northwest of the New Territories combining new towns and village clusters and Sha Tin (ST), a new town area in the Shing Mun River valley were the main hot spots during the daytime in 2006 and kept warmer in the following ten years. The New Territories appeared to see a warming spread in the daytime through its whole northern part and connect to the core urban areas. New towns in the northern part of the New Territories remained the hot spots in the nighttime. Compared with the built-up areas, major country park areas like Tai Mo Shan (TMS) in the New Territories, Tai Tam (TT) on Hong Kong Island, and Lantau South (LS) stay relatively cooler in both the daytime and nighttime during the whole study period, although the VHDHs and HNHs still elevated to some extent under the warming context. Overall, the extreme hot weather during both the daytime and nighttime in Hong Kong's summer had greatly increased over the ten-year span. Hot spots were somewhat different between daytime and nighttime. The core urban areas in Kowloon and Hong Kong Island and new towns in the New Territories were the main hot spots in the nighttime. However, besides the core urban areas, the northern part of the New Territories had rapidly turned to be an expanse of hotspots.

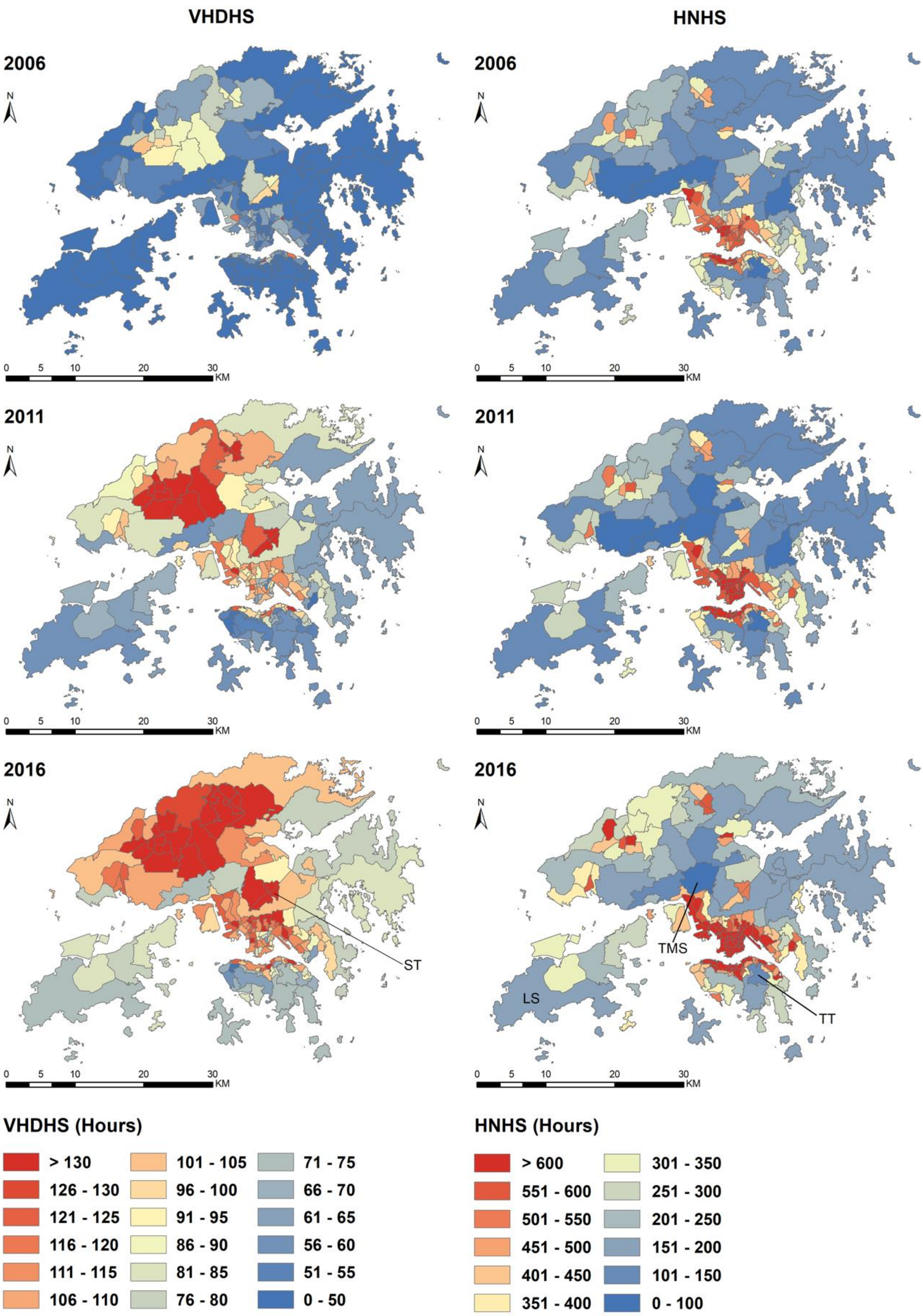

Figure 3. The spatial distribution of heat hazard

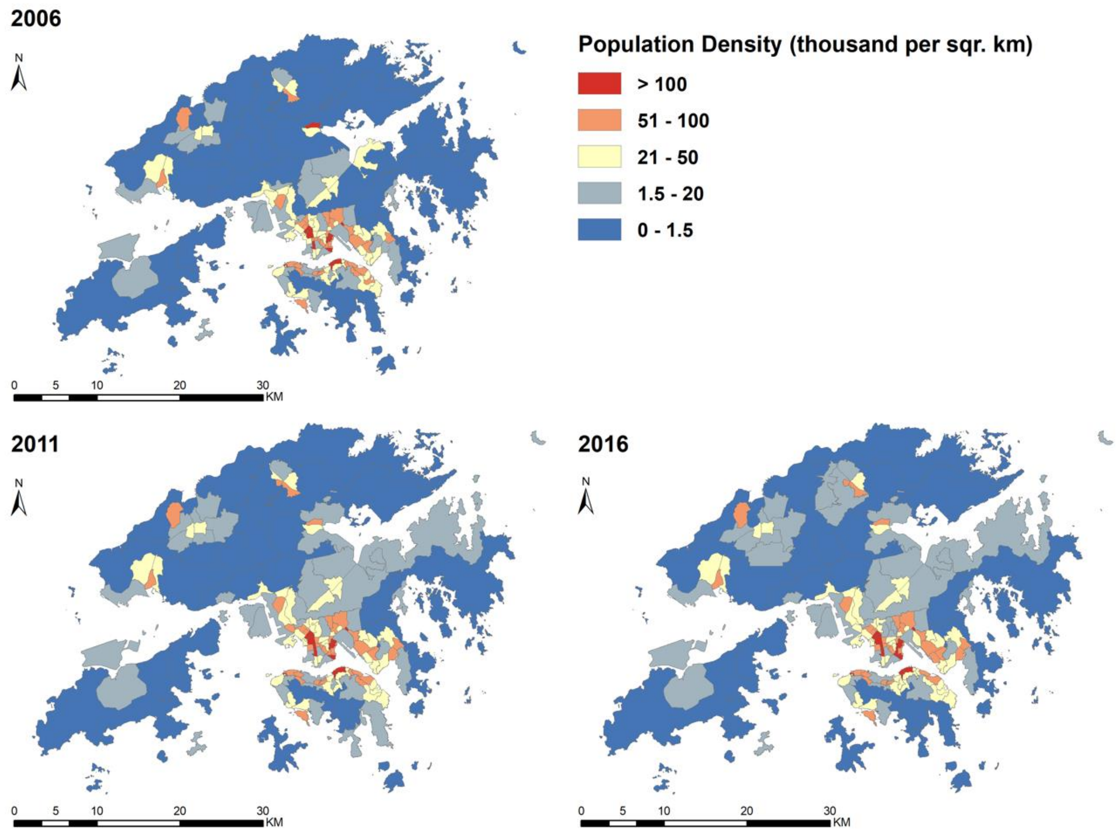

Figure 4. Spatial distribution of population density in Hong Kong

3.3 Heat exposure

The heat exposure of Hong Kong reflected by population density (Figure 4) increased gradually through the ten years and spatially varied. During the study period, the population volume amounted to 6.86 million in 2006 and rose to 7.34 million in 2016 (CenStatD, 2017b). The populations of Hong Kong Island, Kowloon and the New Territories in 2006 (2016) occupied 18.5% (17.1%), 29.4% (30.6%), and 52.1% (52.3%), respectively. The 2016 census results reported a less apparent trend of internal migration to new towns in the New Territories (CenStatD, 2017a) and noted a higher percentage of households (33.8%) in the new towns living in public rental housing and a lower percentage (44.0%) in private permanent housing, compared to the corresponding figures for combined Hong Kong Island and Kowloon (29.9% and 57.9%, respectively). As TPUs are established for town planning purposes, the size of LTPUs varies from 0.09 to 105 km^2, and the population varies from 10 thousand to 280 thousand in the light of internal homogeneities such as estates and country parks. However, large LTPUs as country parks may support small populations, whilst small ones as estates may accommodate large populations. Hence, at the LTPU level, the population density had a large span from less than 1 thousand per km^2 scattered in country parks or the Islands District mainly in the New Territories and the southern part of Hong Kong Island to more than 100 thousand per km^2 concentrated in Kowloon and the northern part of Hong Kong Island. Combining Figure 4 with Figure 3, the spatial distribution of high population density can be found connected with the high temperature, especially HNHs, which is supposed to be related to the UHI effects.

Table 2. PCA results

	2006		2011		2016	
	PC1	PC2	PC1	PC2	PC1	PC2
Factor loadings						
% Population aged 65 and above	**0.789**	0.101	**0.767**	0.108	**0.776**	0.102
% Population aged 15 and above with low education	**0.944**	-0.050	**0.917**	-0.058	**0.927**	0.006
% Households with low income	**0.919**	0.222	**0.929**	0.140	**0.894**	0.267
% Population in PRH	**0.630**	**-0.657**	**0.717**	-0.496	**0.716**	-0.441
% Households in low-quality quarters	0.147	**0.661**	-0.117	**0.725**	-0.103	**0.778**
% One-person households	0.070	**0.806**	0.240	**0.819**	0.276	**0.759**
Eigenvalue	2.781	1.580	2.875	1.478	2.861	1.457
% Variance explained	0.464	0.263	0.479	0.246	0.477	0.243
Cumulative	0.727		0.726		0.720	
Kaiser-Meyer-Olkin Measure of Sampling Adequacy	0.635		0.663		0.603	
Bartlett Test of Sphericity						
Chi-square	464.543		449.064		461.144	
p-value	0.000		0.000		0.000	

Values over 0.5 or less than -0.5 are bolded.

3.4 Heat vulnerability

The PCA produced nearly constant results containing the PCs' eigenvalues, percentages of variance explained, and loadings (presented in Table 2) across the three models. The data were suitable for the PCA with acceptable KMO measures around 0.6 and passed Bartlett's tests (p-value < 0.001). Two PCs with eigenvalues ≥ 1 were eventually returned to jointly explain about 72% of the overall variance. According to the rotated component matrixes, PC1was mainly related to low education, low income, the elderly, and public rental housing, and PC2 was featured with living alone and low-quality quarters. The percentage of the population living in public rental housing had high but opposite loadings for PC1 and PC2, indicating that public rental housing and low-quality quarters were mutually exclusive in most LTPUs.

The heat vulnerability maps of 2006, 2011 and 2016 are shown in Figure 5. The integrated vulnerability index was categorized into 5 classes in ArcGIS 10.6 to represent 5 vulnerability levels. The overall distribution of the vulnerability index was relatively stable over time, but the spatial distribution was variant. The vulnerability was generally higher in some patches in the core urban areas, the northern part of the New Territories, and the Islands District throughout the study period. They were characteristics by relatively higher percentages of elderly, less-educated, and low-income populations in common. However, the northern part of the New Territories mixing rural and suburban areas was also featured with a high proportion of low-quality quarters. Some islands in the south of Hong Kong were also found to be of high vulnerability. In high-density Kowloon, high vulnerability appeared and remained in some LTPUs that were mainly composed of public housing estates in e.g. Sham Shui Po (SSP, LTPU-265), Ho Man Tin Estate (HMTE, LTPU-237), Wong Tai Sin (WTS, LTPU-283), and Choi Hung (CH, LTPU-287), where the proportions of low-income households were also relatively higher accordingly. In 2016, a patch (LTPU-325) in Tsuen Wan combining old industrial buildings, public housing estates, temporary quarters, and old residences turned to be highly vulnerable. Low vulnerability occurred in both country parks and the core urban areas. There was a relatively low-vulnerability area in the center of the Kowloon Peninsula in 2016, which roughly covers Kowloon Tsai and Kowloon Tong (KT-KT, LTPUs-271 & 272). Although the patch has been affected by high temperatures in summer in the center of Kowloon, as an affluent residential area, the heat vulnerability was lowered by residents' high socioeconomic status and high living quality.

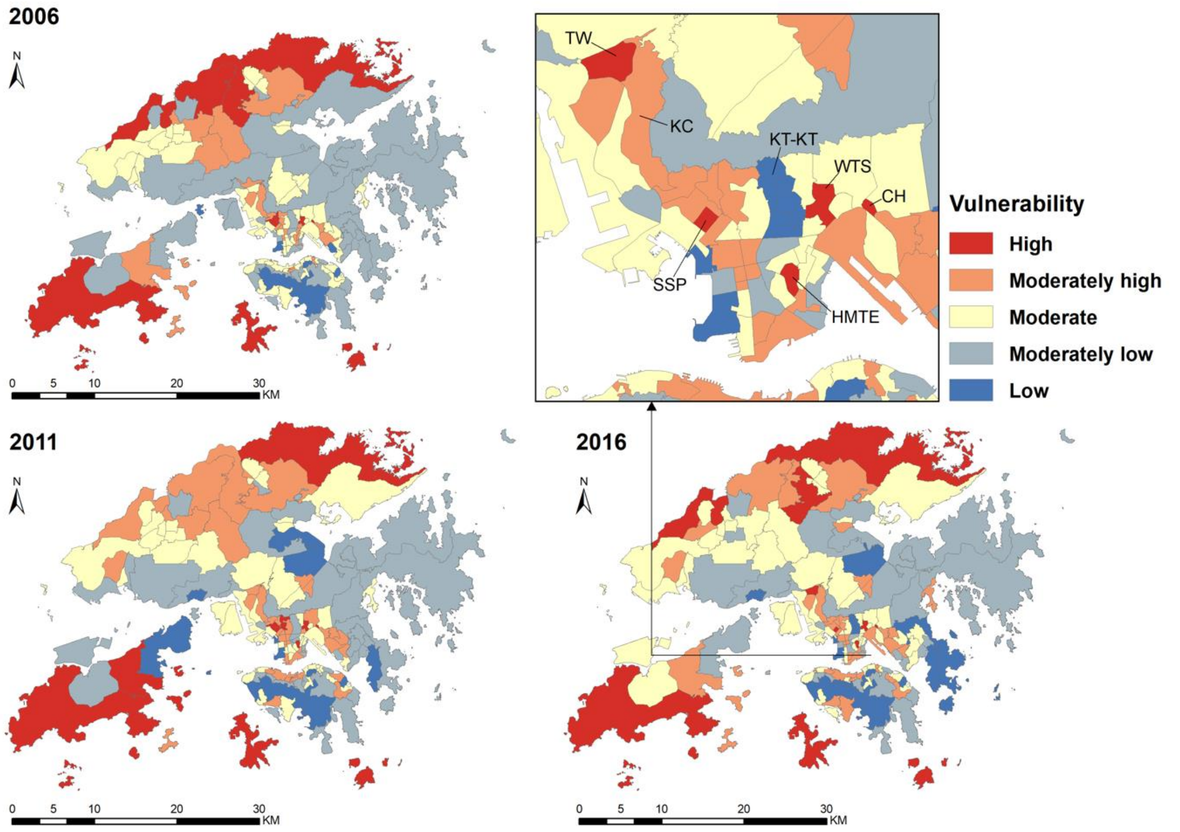

Figure 5. Spatial distribution of vulnerability levels in Hong Kong

3.5 Heat risk combining heat hazard, exposure, and vulnerability

Heat risk maps are of more actual implications because they can highlight the LTPUs of high hazard, exposure, and vulnerability. We produced heat risk maps of 2006, 2011 and 2016 by overlaying the heat hazard, exposure, and vulnerability layers by study year. Given that risk mitigation resources may be limited, a relative ranking of the daytime/nighttime heat risk at the LTPU level for each study year would be more informative based on the standardized scores, so we categorized the risk scores into five levels for each year. The mapping results at the LTPU scale demonstrate some hot spots of high heat risk in Hong Kong.

As is shown in Figure 6, in the daytime, relatively high heat risks happened in the northern part of the New Territories mixing suburban areas, rural areas, and new towns, several new towns like Sha Tin and Tsuen Wan, and the core urban areas including the northern part of Hong

Kong Island and Kowloon. The top risk spots were found to be in Sham Shui Po (LTPU-266, Yau Ma Tei (YMT, LTPU-228), Mong Kok (MK, LTPU-229) and Choi Hung (LTPU-287) throughout the ten years. Two patches separately in Wan Chai (LTPU-132) and the city center of Sha Tin (LTPU-755) should be also concerned as the former was once at the high risk level in 2006 and 2011, while the latter grew to be a hot spot in 2016.

The number of high-risk spots increased from daytime (5, 6 and 7) to nighttime (13, 14 and 16) in respective years with nearly 10 more hot spots in the core urban areas in the nighttime. In the nighttime, heat risks in suburban areas lowered down, while the core urban areas and the new towns were still faced with relatively high heat risks. The daytime hot spots in Kowloon held at high-level risk in the nighttime. Nighttime hot spots in 2016 appeared not only in Sham Shui Po (LTPUs-265, 266 & 267), Yau Ma Tei (YMT, LTPUs-225 & 228), and Choi Hung (LTPU-287) but also in Mong Kok (LTPUs-227, 229 & 221), Wong Tai Sin (LTPU-283), and To Kwa Wan (TKW, LTPUs-241, 242 & 243) in Kowloon and several communities in the Central and Western (LTPU-116 & 113-114) and Wan Chai (LTPU-132) on Hong Kong Island. High-risk LTPUs in Sham Shui Po, Mong Kok, and Yau Ma Tei connected into one large area. Some new towns in the New Territories should also be noted: Tai Po (TP) and Tsuen Wan kept at the moderately high nighttime risk from 2006 to 2016, and Sha Tin, Tuen Mun (TM), and Tin Shui Wai (TSW) in 2016 were at higher nighttime risk in 2016 than before. Low-risk areas in the nighttime were mainly areas covering large country parks or undeveloped lands. Throughout the six maps, we found the high-level heat risk was mainly concentrated on some spots in the core urban areas and the relative risk levels dynamically fluctuated for some areas across time and presented different patterns between daytime and nighttime.

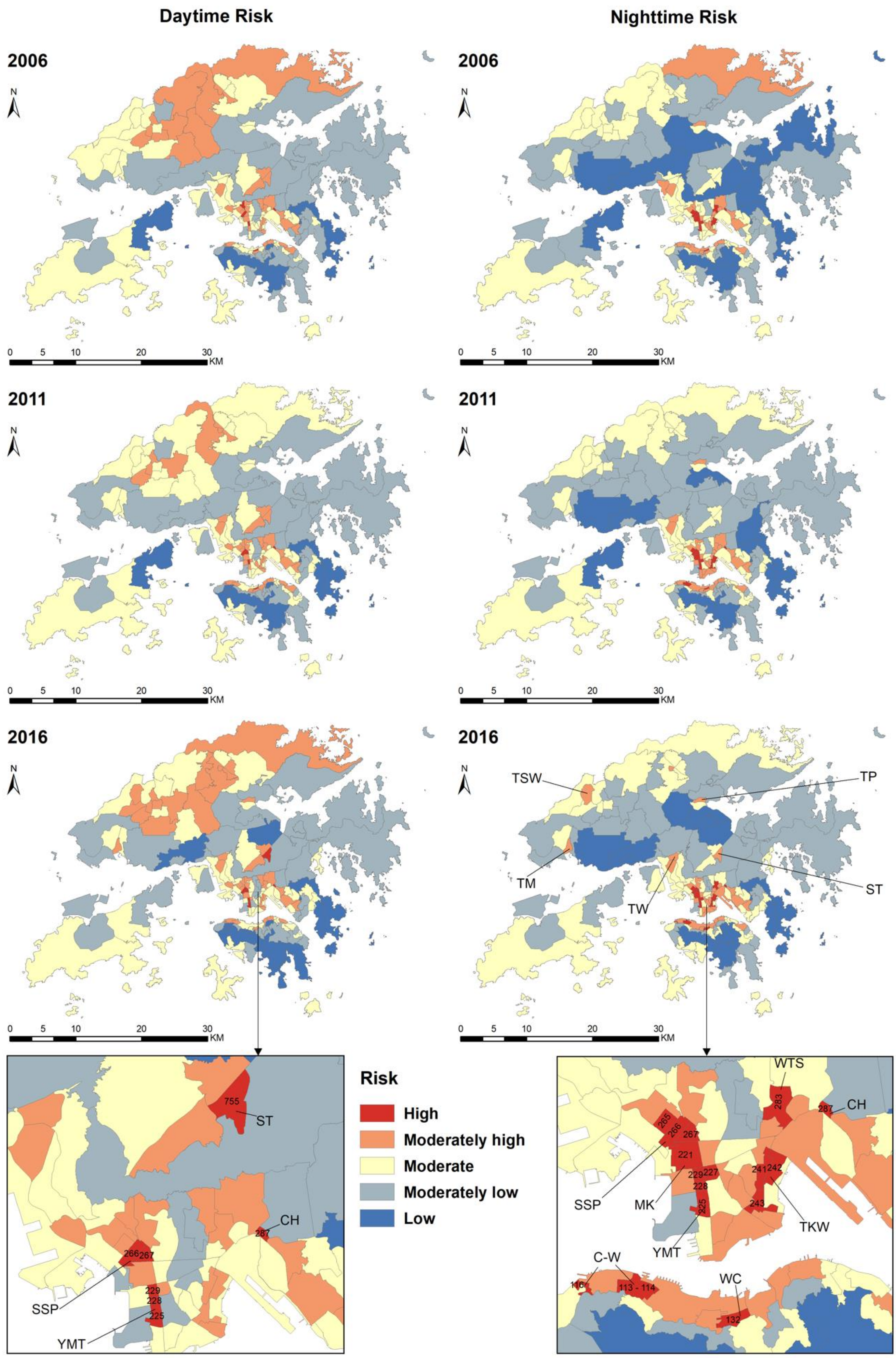

Figure 6. Heat risk maps of Hong Kong

4. Discussion

4.1 Nighttime and daytime heat risks

Our study results reveal that extreme hot weather conditions of Hong Kong have been worsening in both the daytime and nighttime in the recent decade. Some communities remained at a high risk level during daytime or nighttime, especially those in the core urban areas (Kowloon and the northern part of the Hong Kong Island). There are some differences in the spatial distribution of the heat risk between daytime and nighttime. Some relatively less built-up areas in the northern part of the New Territory would experience night cooling, which made their heat hazard much lower in the nighttime than that in the daytime. However, for the core urban areas, the relatively high daytime hazard and risk remained or even became higher in the nighttime. Some communities in the core urban Kowloon kept at high risks all day. Six out of seven hot spots with a high-risk level in the daytime still had a high-risk level in the nighttime except the one in Sha Tin in the New Territories. Moreover, the number of LTPUS with the high-level risk in the nighttime was found to be greater than that in the daytime, and some nighttime hot spots were connected, both calling for a special attention to the nighttime hot spots. Jacobs et al. (2019) also found different patterns of outdoor exposure between day and night in three South Asian cities and informal neighborhoods remained warm during nighttime. Nighttime extreme heat events may cause a more significant health impact (Ho et al., 2017; Wang et al., 2019). Hong Kong's dense built-environment could hinder the urban areas from cooling down in the nighttime in summer (Shi et al., 2018). Heat preservation fueled by UHI, particularly atmospheric UHI, helps keep the urban areas continuously hot during the nighttime (Oke et al., 2017). Consecutive hot nights (≥ 28°C) combined with very hot days (≥ 33°C) including three or five consecutive hot nights (Ho et al., 2017) and consecutive three hot nights and two very hot days (Wang et al., 2019) have been found positively associated with higher mortality risks in the context of Hong Kong, especially for the elderly. On the basis of an understanding of the spaciotemporal distribution of the extreme heat risk, it's necessary to find out the hidden contributors in the next step for targeted risk reduction.

4.2 Analysis of the underlying determinants behind those hot spots at a high-risk level

4.2.1 LTPUs with a high-risk level

The underlying risk determinants including hazard, exposure, and vulnerability vary across the high-risk spots. The bottom of Figure 6 zooms in for the hot spots with the high-risk level in the daytime and nighttime in the most recent 2016 as an illustration. The detailed results are presented in Supplementary Materials. In the daytime, the population density of all the seven LTPUs except the one in Sha Tin (LTPU-755) was over 110 thousand people per km^2, as the dominant contributor to the high risk of the LTPUs in Sham Shui Po, Mong Kok, Yau Ma Tei, and Choi Hong in Kowloon. Sha Tin, as a new town, is not as densely populated as the core urban areas. The hot spots in Sha Tin and Choi Hong were in the top lists of the daytime extreme heat hazard and the vulnerability component combing the elderly, low education and income, and public rental housing. In the nighttime, 11 hot spots were featured with a very high population density, among which, four LTPUs in Mong Kok (LTPUs-221, 227, 229) and Yau Ma Tei (LTPU-228) had very high levels of nighttime heat hazard. Nighttime heat hazard and the vulnerability component related to social isolation and low-quality housing were main determinants for LTPUs 113-114 and 132 on Hong Kong Island, which, however, only had average levels of population density. Besides the high-risk spot in Choi Hong, two separately in Sham Shui Po (LTPU-265) and Wong Tai Sin (LTPU-283) were also characteristic with the high vulnerability associated with the elderly, low education and income, and public rental housing. Overall, for the year of 2016, high population exposure was a main contributor to the high-risk level of most hot-spots. The two vulnerability factors separately mattered in different LTPUs. Some communities suffered from a particularly high degree of the extreme hot weather hazard. Therefore, targeted risk mitigation measures and strategies in various areas, including urban planning and air ventilation, public education/awareness, information dissemination, heat prevention, urban greening/open spaces, special health care and subsidies for underprivileged, should be considered.

4.2.2 Core urban areas and new towns

In built-up urban areas, land surface morphology is one of the most influential determinants of the extreme heat hazard. It has been observed that some high-rise building areas keep being hotspots of heat hazard both daytime and nighttime. This could be attributed to a combination of causes, including (1) The densely built-up areas have more buildings which release more anthropogenic heat. This is particularly considerable in hot and humid subtropical areas like Hong Kong due to the higher usage rate of air conditioning for cooling during summertime (Wang et al., 2018); (2) In the densely built-up areas, the significantly larger building volume absorbs more shortwave solar radiation from the sky during the daytime and thus stores more heat. During the nighttime, the heat is released from the building blocks in the form of longwave radiation. However, it cannot go back directly to the sky as it is trapped by the dense buildings and narrow street canyon (Giridharan et al., 2007); (3) Relatively lower wind speed in the densely built-up areas could reduce the ventilation required for cooling the city (Peng et al., 2018); (4) The lack of enough green space in the urban center also, to a certain extent, contributes to the situation (Ng et al., 2012).

In Hong Kong, a greater attention should be paid to those high-dense urban areas, which are dichotomously separated into the core urban areas in Kowloon and the northern part of Hong Kong Island and new towns in the New Territories. The highest risk was mainly distributed in the core urban areas. The results are consistent with empirical evidence in the United States

(Reid et al., 2009), Europe (Morabito et al., 2015; Tomlinson et al., 2011; Verdonck et al., 2019), and other cities in China (Dong et al., 2014; W. Zhang et al., 2019). Hence, the top priority should be given to the core urban areas, especially some old communities in Kowloon. The core urban areas of Hong Kong, as one of the densest places in the world, standing high-density and high-rise urban form, but lacking urban green spaces, are faced with not only the high exposure to heat but also the more striking extreme heat events in summer owing to the intensified UHI effect (Shi, Katzschner, & Ng, 2018; M. S. Wong et al., 2016). However, the areas are comprised of a number of small-size highly developed patches (TPUs) with diverse social characteristics, which means some of them may be more vulnerable to extreme hot weather and therefore at greater risks. Some neighborhoods that were almost public housing estates with higher proportions of low-income households in Kowloon are typical examples.

The situation is a little different for the new towns in the New Territories. Due to the limited land use capacity of the city, a total of twelve new towns have been successively built in the New Territories since the 1970s. According to the 2016 census, the population of the twelve new towns in total increased 6.1% over the ten years, reaching 3.44 million in 2016, which occupied 46.9% of the total population of Hong Kong. Some new towns like Sha Tin, Tuen Mun, Tin Shui Wai, and Tai Po showed gradually rising heat risk in either the daytime or the nighttime over the ten years and signs to be emerging hot-spots in the near future mainly because of the fast climbing extreme heat hazard in these built-up areas. Similar phenomenon for satellite cities around city centers has also been recognized in North America (Ho et al., 2018; Wilson & Chakraborty, 2019). The proportion of the elderly increased in new towns (CenStatD, 2017d) where public rental housing was one of major housing types, which also pushed up the vulnerability of the areas. Even so, the densities of the population and the built environment in the new towns are still lower than those in the core urban area. As recently developed, the new towns offer comparably sounder infrastructures such as green spaces that could help mitigate the risk from summer heat. The cooling effect (Lu et al., 2017) has been verified in the core urban areas of Hong Kong by Ng, Chen, Wang, and Yuan (2012). Furthermore, the surrounding country parks could alleviate the UHI effect in the isolated, compact new towns to some extent.

4.2.3 Sub-urban areas

The Islands District and the northern part of the New Territories (excluding new towns) told another story, where villages and country parks dominate. The small population (more than 100,000) and the large territory make the average population density less than 1 thousand per km2. However, the proportions of residents in low socioeconomic status with regard to education, income, and solitude and the elderly in some LTPUs were comparatively higher than other parts of the city, which pushed up the vulnerability levels. The Islands District occupies a large area containing a number of islands with varied area and population. A LTPU of high vulnerability in the south of Hong Kong covers several islands. Some were truly of high vulnerability due to the relatively high percentages of the elderly or one-person households, like Lantau South, whereas some have a fairly small or no population, like Po Tai. Another example is the island of Cheung Chau with a population of over 20 thousand in the area of 2.46 km^2. It topped the percentage of population aged 15 and above with low education at about 36% over the city. Despite the moderately high risk, such the large group of vulnerable dwellers deserve extra attention under the overall warming context.

4.3 Limitations

In spite of some innovations and new knowledge, several limitations in this study are clarified below. The first is the application of the LTPU as the basic spatial unit, but the size and the population of the LTPUs varies. In the core urban areas, the LTPUs are small so that they can approximately represent communities. In the New Territories, there are two situations. The new towns were circled with clear boundaries. However, some LTPUs are large but with small populations, which covers country parks and small scattered settlements. As the system is developed for urban planning, LTPUs are demarcated by geographic features like roads or waterways. It is, therefore, assumed that the environment within a LTPU is relatively homogeneous. The system has been successfully used in local research (Goggins et al., 2012; M. S. Wong et al., 2016). Secondly, the application of the LTPU scale limited the availability of demographic and socioeconomic data. As a consequence, the vulnerability index was developed based on the attainable six indicators. Next, in order to more precisely define the percentage of low-income households in the process of the vulnerability index development, approximate values were adopted as the time-varying thresholds for the indicator due to the discrepancy between the definition of the poverty line and the segmentation of household income level. Even so, we believe it would be better than simply using a simple and constant threshold as suggested by Cutter and Finch (2008). Thirdly, due to the limited availability of demo-socioeconomic data from CenStatD for the three reference years, only the qualitative trend on the temporal variation of the heat vulnerability and risk was presented. Lastly, heat hazard, exposure, and vulnerability equally contributed to heat risk because there has been no standard on weight assignment under the risk triangle framework and the equal weighting scheme has been generally applied (Chen et al., 2018; Ho et al., 2015; W. Zhang et al., 2019). Next-step studies should pursue new approaches and knowledge to more scientifically determine and adjust the importance of each component, particularly on a case-by-case basis.

5. Conclusions

This study has elucidated a spatiotemporal assessment of extreme heat risk at the community scale in the context of a high-density megacity, Hong Kong, for 2006, 2011, and 2016, by developing an extreme heat risk index through quantifying and integrating heat-related hazard, exposure, and vulnerability. The vulnerability was calculated based on the principal component analysis of six demographic and socioeconomic characteristics with regard to the elderly, education, income, and housing status. The five-year average of the annual cumulative very hot day hours and hot night hours in summer were adopted to respectively illustrate daytime and nighttime heat hazard. The heat risk index together with the heat hazard, exposure, and vulnerability was mapped at the LTPU scale. Hot spots of extreme heat risk have been identified among about 150 census patches with underlying determinants. Hot spots with a high-level heat risk were found mainly in core urban areas but somewhat different between daytime and nighttime. High-risk spots were concentrated in some communities in Sham Shui Po, Yau Ma Tei, Mong Kok, and Choi Hung in the core urban Kowloon during both the daytime and the nighttime from 2006 to 2016. For some communities in the core urban areas, the relatively high daytime risk remained or even became higher in the nighttime. All the daytime hot spots in Kowloon remained to be at a high-risk level in the nighttime in 2016. Nearly 10 more high-risk spots in the core urban areas were found in the nighttime than those in the daytime in the three study years. Nighttime hot spots included some extra communities in Wong Tai Sin and To Kwa Wan in Kowloon and the Central and Western and Wan Chai on Hong Kong Island. Some new towns in the New Territories turned to be at higher risk in 2016, especially Sha Tin in the daytime. In terms of underlying determinants behind hot spots, high population exposure was a main factor for the high-risk level of most hot spots. The daytime extreme hot weather hazard mattered for the communities in Sha Tin and Choi Hong, whereas the nighttime hazard was a major contributor for the high risk in communities on the Hong Kong Island and in Yau Ma Tei and Mong Kok. The high risk in four communities separately in Sha Tin, Choi Hong, Sham Shui Po, and Wong Tai Sin was closed related to the high-level of the vulnerability factor representing the elderly, low socioeconomic status and public rental housing. Two high-risk communities on the Hong Kong Island were featured with a greater vulnerability caused by a higher proportion of people living alone and in low-quality quarters.

The study provides methodological and practical implications for heat assessment research and autochthonic heat risk mitigation, respectively. By adopting the Crichton's Risk Triangle approach, three key elements, hazard, exposure, and vulnerability, were jointly taken into account. Station-measured hourly temperature data were utilized to capture and depict the intracity variation of the heat hazard at the fine scale for daytime and nighttime with the technique of land use regression. The approach could reduce the biases and uncertainties caused by the direct extraction of the weather data from the closest stations and therefore improve the robustness of the risk assessment (Ren et al., under preparation). The methodological experience could be used for references in the neighboring cities. As the initial comprehensive assessment of extreme heat risk for the high-density city in East Asia, the present study offers explicit spatial information about the hot spots of heat-related vulnerability and risk which could serve as useful references for relevant decision makers and stakeholders at different levels in formulating measures and strategies to mitigate or avoid possible negative effects of extreme heat in targeted zones or communities (Buscail et al., 2012), for example, provision of heat health information or advisory (X. Zhang et al., 2019), promoting public awareness, special health care, urban greening/open spaces, and subsidies for underprivileged. The results would also be useful for the future assessment and scientific research on sustainable risk mitigation schemes and urban planning targeting neighborhoods of high heat risk with a view to precisely deal with specific vulnerability drivers, informing local adaptation resource allocation, reducing anthropogenic impacts on heat risk increase, and improving public health under the complex context of the metropolis. This study provides feasible empirical evidence for spatially assessing heat risk in high-density cities in terms of demo-socioeconomic determinants, comparison of daytime and nighttime, and differences between downtown areas and dispersed new towns. Other Asia-Pacific large cities in tropical and sub-tropical climate regions such as Taipei, Shenzhen, Guangzhou, Singapore, Delhi, and Kuala Lumpur with high-density urban settings and population may have potential high heat risks with the rising extreme heat. Our study provides a scientific methodology that could be adopted to carry out spatiotemporal assessments of extreme heat risk from the perspective of environmental and socioeconomic perspectives for these cities.

Future research is expected to establish a framework involving multi-dimensional and multi-disciplinary theories and factors for spatial assessment of heat risk of high-density cities. More knowledge like wind environment could be integrated for more accurate estimation of heat risk in urban contexts. High-rise and high-density morphology may make the wind environment complicated at the community or even street block level (Lai et al., 2014; Ng et al., 2011; Peng et al., 2018), but the increasing urban ventilation could help mitigate the UHI effect and improve human thermal comfort condition of citizens (Rajagopalan et al., 2014). Based on the scientific risk assessment, evidence-based climate responsive strategies, planning, and actions, e.g. developing spatially explicit services for heat risk mitigation (Keramitsoglou et al., 2017) and using cool materials to increase building surface reflectivity for reducing the UHI effect in high-density built-up areas (Castellani et al., 2017; Morini et al., 2018), can be enacted and conducted for raising the adaptation, sustainability, and resilience of high-density cities.

Ethics approval and consent to participate: Not applicable

Consent for publication: Not applicable

Availability of data and material

The meteorological data and the demo-socioeconomic data that support the findings of this study are available respectively from the Hong Kong Observatory and the Census and Statistics Department of Hong Kong SAR but need to apply for research purpose. Results are available from the authors upon request and with permission of the project partners.

Competing interests: We know of no conflicts of interest associated with this publication.

Funding:

The study is supported by The Vice-Chancellor's Discretionary Fund of The Chinese University of Hong Kong. It is also funded by a General Research Fund Project Grant 2017-18 (Ref No.: RGC-GRF 14611517, named "Climatic-responsive planning and action for mitigating heat-related health risk at the community level in high-density cities– A Case of Hong Kong ") and Research Impact Fund 2018-19 (Ref No: R4046-18, named 'Increasing the Resilience to the Health Impacts of Extreme Weather on Older People under Future Climate Change') of Hong Kong Research Grants Council.

Acknowledgments

This study is a collaborative research project among three research teams from The University of Hong Kong, The Chinese University of Hong Kong, and the Hong Kong Observatory. Authors would like to thank the Hong Kong Observatory and the Census and Statistics Department of Hong Kong SAR for providing meteorological data and demo-socioeconomic data, respectively.

References

Aflaki, A., Mirnezhad, M., Ghaffarianhoseini, A., Ghaffarianhoseini, A., Omrany, H., Wang, Z.-H., & Akbari, H. (2017). Urban heat island mitigation strategies: A state-of-the-art review on Kuala Lumpur, Singapore and Hong Kong. *Cities, 62*, 131-145. doi:10.1016/j.cities.2016.09.003

Aminipouri, M., Knudby, A., & Ho, H. C. (2016). Using multiple disparate data sources to map heat vulnerability: Vancouver case study. *The Canadian Geographer / Le Géographe canadien, 60*(3), 356-368. doi:10.1111/cag.12282

Åström, D. O., Bertil, F., & Joacim, R. (2011). Heat wave impact on morbidity and mortality in the elderly population: a review of recent studies. *Maturitas, 69*(2), 99-105. doi:10.1016/j.maturitas.2011.03.008

Aubrecht, C., & Ozceylan, D. (2013). Identification of heat risk patterns in the U.S. National Capital Region by integrating heat stress and related vulnerability. *Environment International, 56*, 65-77. doi:10.1016/j.envint.2013.03.005

Bakhsh, K., Rauf, S., & Zulfiqar, F. (2018). Adaptation strategies for minimizing heat wave induced morbidity and its determinants. *Sustainable Cities and Society, 41*, 95-103. doi:https://doi.org/10.1016/j.scs.2018.05.021

Bao, J., Li, X., & Yu, C. (2015). The Construction and Validation of the Heat Vulnerability Index, a Review. *International Journal of Environmental Research and Public Health, 12*(7), 7220-7234. doi:10.3390/ijerph120707220

Basu, R. (2009). High ambient temperature and mortality: a review of epidemiologic studies from 2001 to 2008. *Environ Health, 8*, 40. doi:10.1186/1476-069X-8-40

Bradford, K., Abrahams, L., Hegglin, M., & Klima, K. (2015). A Heat Vulnerability Index and Adaptation Solutions for Pittsburgh, Pennsylvania. *Environmental Science & Technology, 49*(19), 11303-11311. doi:10.1021/acs.est.5b03127

Buscail, C., Upegui, E., & Viel, J.-F. (2012). Mapping heatwave health risk at the community level for public health action. *International Journal of Health Geographics, 11*(1), 38. doi:10.1186/1476-072X-11-38

Castellani, B., Morini, E., Anderini, E., Filipponi, M., & Rossi, F. (2017). Development and characterization of retro-reflective colored tiles for advanced building skins. *Energy and Buildings, 154*, 513-522. doi:https://doi.org/10.1016/j.enbuild.2017.08.078

CenStatD. (2017a). *2016 Population By-census Main Results*. Retrieved from https://www.statistics.gov.hk/pub/B11200982016XXXXB0100.pdf

CenStatD. (2017b). *Demographic Trends in Hong Kong 1986-2016*. Retrieved from https://www.statistics.gov.hk/pub/B1120017042017XXXXB0100.pdf

CenStatD. (2017c). *Hong Kong 2016 Population By-census - Thematic Report: Household Income Distribution in Hong Kong*. Retrieved from Hong Kong: https://www.statistics.gov.hk/pub/B11200962016XXXXB0100.pdf

CenStatD. (2017d). *Hong Kong 2016 Population By-census - Thematic Report: Older Persons*. Retrieved from Hong Kong: https://www.statistics.gov.hk/pub/B11201052016XXXXB0100.pdf

CenStatD. (2017e). *Hong Kong Population Projection 2017-2066*. Retrieved from Hong Kong: https://www.statistics.gov.hk/pub/B1120015072017XXXXB0100.pdf

CenStatD. (2019a, Sep 24, 2019). 2011 Population Census - Concepts and Methods. Retrieved from https://www.censtatd.gov.hk/hkstat/sub/sc170.jsp

CenStatD. (2019b). *Hong Kong Poverty Situation Report 2018*. Retrieved from Hong Kong: https://www.statistics.gov.hk/pub/B9XX0005E2018AN18E0100.pdf

Cerin, E., Sit, C. H., Zhang, C. J., Barnett, A., Cheung, M. M., Lai, P.-c., . . . Lee, R. S. (2016). Neighbourhood environment, physical activity, quality of life and depressive symptoms in Hong Kong older adults: a protocol for an observational study. *BMJ open, 6*(1), e010384.

Chan, E. Y., Goggins, W. B., Kim, J. J., & Griffiths, S. M. (2012). A study of intracity variation of temperature-related mortality and socioeconomic status among the Chinese population in Hong Kong. *J Epidemiol Community Health, 66*(4), 322-327. doi:10.1136/jech.2008.085167

Chan, E. Y. Y., Goggins, W. B., Kim, J. J., Griffiths, S., & Ma, T. K. (2011). Help-seeking behavior during elevated temperature in Chinese population. *Journal of Urban Health, 88*(4), 637.

Chau, P. H., Chan, K. C., & Woo, J. (2009). Hot weather warning might help to reduce elderly mortality in Hong Kong. *International Journal of Biometeorology, 53*(5), 461-468. doi:10.1007/s00484-009-0232-5

Chen, G., Li, S., Knibbs, L. D., Hamm, N. A. S., Cao, W., Li, T., . . . Guo, Y. (2018). A machine learning method to estimate PM2.5 concentrations across China with remote sensing, meteorological and land use information. *Science of the Total Environment, 636*, 52-60. doi:https://doi.org/10.1016/j.scitotenv.2018.04.251

Crichton, D. (1999). The risk triangle. In J. Ingleton (Ed.), *Natural Disaster Management* (pp. 102-103). Leicester, UK: Tudor Rose Holdings Limited.

Cutter, S. L., & Finch, C. (2008). Temporal and spatial changes in social vulnerability to natural hazards. *Proceedings of the National Academy of Sciences, 105*(7), 2301. doi:10.1073/pnas.0710375105

Dong, W., Liu, Z., Zhang, L., Tang, Q., Liao, H., & Li, X. e. (2014). Assessing heat health risk for sustainability in Beijing's urban heat island. *Sustainability, 6*(10), 7334-7357. doi:10.3390/su6107334

Dunn, J. R. (2000). Housing and health inequalities: review and prospects for research. *Housing Studies, 15*(3), 341-366.

Estoque, R. C., Ooba, M., Seposo, X. T., Togawa, T., Hijioka, Y., Takahashi, K., & Nakamura, S. (2020). Heat health risk assessment in Philippine cities using remotely sensed data and social-ecological indicators. *Nat Commun, 11*(1), 1581. doi:10.1038/s41467-020-15218-8

Gasparrini, A., Guo, Y., Hashizume, M., Lavigne, E., Zanobetti, A., Schwartz, J., . . . Armstrong, B. (2015). Mortality risk attributable to high and low ambient temperature: a multicountry observational study. *The Lancet, 386*(9991), 369-375. doi:10.1016/s0140-6736(14)62114-0

Giridharan, R., Lau, S. S. Y., Ganesan, S., & Givoni, B. (2007). Urban design factors influencing heat island intensity in high-rise high-density environments of Hong Kong. *Building and Environment, 42*(10), 3669-3684. doi:https://doi.org/10.1016/j.buildenv.2006.09.011

Goggins, W. B., Chan, E. Y., Ng, E., Ren, C., & Chen, L. (2012). Effect modification of the association between short-term meteorological factors and mortality by urban heat islands in Hong Kong. *PloS One, 7*(6), e38551. doi:10.1371/journal.pone.0038551

Gronlund, C. J. (2014). Racial and socioeconomic disparities in heat-related health effects and their mechanisms: a review. *Curr Epidemiol Rep, 1*(3), 165-173. doi:10.1007/s40471-014-0014-4

Gronlund, C. J., Berrocal, V. J., White-Newsome, J. L., Conlon, K. C., & O'Neill, M. S. (2015). Vulnerability to extreme heat by socio-demographic characteristics and area green space among the elderly in Michigan, 1990-2007. *Environmental Research, 136*, 449-461. doi:10.1016/j.envres.2014.08.042

Guo, Y., Gasparrini, A., Li, S., Sera, F., Vicedo-Cabrera, A. M., de Sousa Zanotti Stagliorio Coelho, M., . . . Tong, S. (2018). Quantifying excess deaths related to heatwaves under climate change scenarios: A multicountry time series modelling study. *PLoS Medicine, 15*(7), e1002629. doi:10.1371/journal.pmed.1002629

HKO. (2020a). Climate Change in Hong Kong - Extreme weather events. Retrieved from https://www.hko.gov.hk/en/climate_change/obs_hk_extreme_weather.htm

HKO. (2020b). Monthly Meteorological Normals for Hong Kong. Retrieved from https://www.hko.gov.hk/en/cis/normal/1981_2010/normals.htm

HKO. (2020c). Monthly Weather Summary of July 2020. Retrieved from https://www.hko.gov.hk/en/wxinfo/pastwx/mws2020/mws202007.htm

Ho, H. C., Knudby, A., Chi, G., Aminipouri, M., & Lai, D. Y. (2018). Spatiotemporal analysis of regional socio-economic vulnerability change associated with heat risks in Canada. *Appl Geogr, 95*, 61-70. doi:10.1016/j.apgeog.2018.04.015

Ho, H. C., Knudby, A., & Huang, W. (2015). A Spatial Framework to Map Heat Health Risks at Multiple Scales. *International Journal of Environmental Research and Public Health, 12*(12), 16110-16123. doi:10.3390/ijerph121215046

Ho, H. C., Lau, K. K., Ren, C., & Ng, E. (2017). Characterizing prolonged heat effects on mortality in a sub-tropical high-density city, Hong Kong. *International Journal of Biometeorology, 61*(11), 1935-1944. doi:10.1007/s00484-017-1383-4

Hoek, G., Beelen, R., de Hoogh, K., Vienneau, D., Gulliver, J., Fischer, P., & Briggs, D. (2008). A review of land-use regression models to assess spatial variation of outdoor air pollution. *Atmospheric Environment, 42*(33), 7561-7578. doi:10.1016/j.atmosenv.2008.05.057

Hu, K., Yang, X., Zhong, J., Fei, F., & Qi, J. (2017). Spatially Explicit Mapping of Heat Health Risk Utilizing Environmental and Socioeconomic Data. *Environmental Science & Technology, 51*(3), 1498-1507. doi:10.1021/acs.est.6b04355

IBM Corp. (2019). IBM SPSS Statistics for Windows, Version 26.0. Armonk, NY: IBM Corp.

IPCC. (2014). *Climate Change 2014: Impacts, Adaptation and Vulnerability. Part A: Global and Sectoral Aspects. Contribution of Working Group II to the Fifth Assessment Report of the Intergovernmental Panel on Climate Change* (C. B. Field, V. R. Barros, D. J. Dokken, K. J.

Mach, M. D. Mastrandrea, T. E. Bilir, M. Chatterjee, K. L. Ebi, Y. O. Estrada, R. C. Genova, B. Girma, E. S. Kissel, A. N. Levy, S. MacCracken, P. R. Mastrandrea, & L. L. White Eds.). Cambridge, UK and New York, NY, USA: Cambridge University Press.

Jacobs, C., Singh, T., Gorti, G., Iftikhar, U., Saeed, S., Syed, A., . . . Siderius, C. (2019). Patterns of outdoor exposure to heat in three South Asian cities. *Science of the Total Environment*, *674*, 264-278. doi:10.1016/j.scitotenv.2019.04.087

Johnson, D. P., Stanforth, A., Lulla, V., & Luber, G. (2012). Developing an applied extreme heat vulnerability index utilizing socioeconomic and environmental data. *Applied Geography*, *35*(1-2), 23-31. doi:10.1016/j.apgeog.2012.04.006

Kaiser, H. F. (1960). The application of electronic computers to factor analysis. *Educational and Psychological Measurement*, *20*(1), 141-151.

Kaźmierczak, A., & Cavan, G. (2011). Surface water flooding risk to urban communities: Analysis of vulnerability, hazard and exposure. *Landscape and Urban Planning*, *103*(2), 185-197. doi:https://doi.org/10.1016/j.landurbplan.2011.07.008

Kenny, G. P., Yardley, J., Brown, C., Sigal, R. J., & Jay, O. (2010). Heat stress in older individuals and patients with common chronic diseases. *Cmaj*, *182*(10), 1053-1060.

Keramitsoglou, I., Sismanidis, P., Analitis, A., Butler, T., Founda, D., Giannakopoulos, C., . . . Kiranoudis, C. T. (2017). Urban thermal risk reduction: Developing and implementing spatially explicit services for resilient cities. *Sustainable Cities and Society*, *34*, 56-68. doi:https://doi.org/10.1016/j.scs.2017.06.006

Klinenberg, E. (2003). Review of heat wave: social autopsy of disaster in Chicago. *New England Journal of Medicine*, *348*(7), 666-667.

Kwok, Y. T., Lai, A. K. L., Lau, K. K.-L., Chan, P. W., Lavafpour, Y., Ho, J. C. K., & Ng, E. Y. Y. (2017). Thermal comfort and energy performance of public rental housing under typical and near-extreme weather conditions in Hong Kong. *Energy and Buildings*, *156*, 390-403. doi:10.1016/j.enbuild.2017.09.067

Lai, S. T. E., Lee, T. C., & H., L. Y. (2014). Winds that help a city to breathe. *Hong Kong Meteorological Society Bulletin*, *24*, 24 – 32.

Lee, K. L., Chan, Y. H., Lee, T. C., Goggins, W. B., & Chan, E. Y. Y. (2015). The development of the Hong Kong Heat Index for enhancing the heat stress information service of the Hong Kong Observatory. *International Journal of Biometeorology*, *60*(7), 1029-1039. doi:10.1007/s00484-015-1094-7

Li, D., & Bou-Zeid, E. (2013). Synergistic Interactions between Urban Heat Islands and Heat Waves: The Impact in Cities Is Larger than the Sum of Its Parts. *Journal of Applied Meteorology and Climatology*, *52*(9), 2051-2064. doi:10.1175/jamc-d-13-02.1

Li, T., Horton, R. M., Bader, D. A., Zhou, M., Liang, X., Ban, J., . . . Kinney, P. L. (2016). Aging will amplify the heat-related mortality risk under a changing climate: projection for the elderly in Beijing, China. *Scientific Reports*, *6*, 28161.

Liu, J., Hansen, A., Varghese, B., Liu, Z., Tong, M., Qiu, H., . . . Bi, P. (2020). Cause-specific mortality attributable to cold and hot ambient temperatures in Hong Kong: a time-series study, 2006–2016. *Sustainable Cities and Society*, 102131. doi:https://doi.org/10.1016/j.scs.2020.102131

Loughnan, M., Carroll, M., & Tapper, N. J. (2015). The relationship between housing and heat wave resilience in older people. *International Journal of Biometeorology*, *59*(9), 1291-1298.

Luber, G., & McGeehin, M. (2008). Climate change and extreme heat events. *American Journal of Preventive Medicine*, *35*(5), 429-435. doi:10.1016/j.amepre.2008.08.021

Macnee, R. G. D., & Tokai, A. (2016). Heat wave vulnerability and exposure mapping for Osaka City, Japan. *Environment Systems and Decisions*, *36*(4), 368-376. doi:10.1007/s10669-016-9607-4

Mora, C., Dousset, B., Caldwell, I. R., Powell, F. E., Geronimo, R. C., Bielecki, C. R., . . . Trauernicht, C. (2017). Global risk of deadly heat. *Nature Climate Change*, *7*(7), 501-+. doi:10.1038/nclimate3322

Morabito, M., Crisci, A., Gioli, B., Gualtieri, G., Toscano, P., Di Stefano, V., . . . Gensini, G. F. (2015). Urban-hazard risk analysis: mapping of heat-related risks in the elderly in major Italian cities. *PloS One*, *10*(5), e0127277. doi:10.1371/journal.pone.0127277

Morini, E., Castellani, B., De Ciantis, S., Anderini, E., & Rossi, F. (2018). Planning for cooler urban canyons: Comparative analysis of the influence of façades reflective properties on urban canyon thermal behavior. *Solar Energy*, *162*, 14-27. doi:https://doi.org/10.1016/j.solener.2017.12.064

Mushore, T. D., Mutanga, O., Odindi, J., & Dube, T. (2017). Determining extreme heat vulnerability of Harare Metropolitan City using multispectral remote sensing and socio-economic data. *Journal of Spatial Science*, *63*(1), 173-191. doi:10.1080/14498596.2017.1290558

Nayak, S. G., Shrestha, S., Kinney, P. L., Ross, Z., Sheridan, S. C., Pantea, C. I., . . . Hwang, S. A. (2018). Development of a heat vulnerability index for New York State. *Public Health*, *161*, 127-137. doi:10.1016/j.puhe.2017.09.006

Ng, E., Chen, L., Wang, Y., & Yuan, C. (2012). A study on the cooling effects of greening in a high-density city: An experience from Hong Kong. *Building and Environment*, *47*, 256-271. doi:https://doi.org/10.1016/j.buildenv.2011.07.014

Ng, E., Yuan, C., Chen, L., Ren, C., & Fung, J. C. H. (2011). Improving the wind environment in high-density cities by understanding urban morphology and surface roughness: A study in Hong Kong. *Landscape and Urban Planning*, *101*(1), 59-74. doi:https://doi.org/10.1016/j.landurbplan.2011.01.004

Oke, T. R., Mills, G., Christen, A., & Voogt, J. A. (2017). *Urban Climates*. Cambridge: Cambridge University Press.

Otto, I. M., Reckien, D., Reyer, C. P. O., Marcus, R., Le Masson, V., Jones, L., . . . Serdeczny, O. (2017). Social vulnerability to climate change: a review of concepts and evidence. *Regional Environmental Change*, *17*(6), 1651-1662. doi:10.1007/s10113-017-1105-9

Peng, L., Liu, J.-P., Wang, Y., Chan, P.-w., Lee, T.-c., Peng, F., . . . Li, Y. (2018). Wind weakening in a dense high-rise city due to over nearly five decades of urbanization. *Building and Environment*, *138*, 207-220. doi:https://doi.org/10.1016/j.buildenv.2018.04.037

PlanD. (2004). *Implementation of Data Alignment Measures for the Alignment of Planning, Lands and Public Works Data. Final Report (Volume 2E). Specification and Explanatory Notes of TPU/SB CSU*. Retrieved from Hong Kong:

PlanD. (2019). Land Utilization in Hong Kong 2018. Retrieved from https://www.pland.gov.hk/pland_en/info_serv/statistic/landu.html

Rajagopalan, P., Lim, K. C., & Jamei, E. (2014). Urban heat island and wind flow characteristics of a tropical city. *Solar Energy*, *107*, 159-170. doi:https://doi.org/10.1016/j.solener.2014.05.042

Reid, C. E., O'Neill, M. S., Gronlund, C. J., Brines, S. J., Brown, D. G., Diez-Roux, A. V., & Schwartz, J. (2009). Mapping community determinants of heat vulnerability. *Environmental Health Perspectives*, *117*(11), 1730-1736. doi:10.1289/ehp.0900683

Ren, C., Wang, K., Shi, Y., Kwok, Y. T., Morakinyo, T. E., Lee, T. C., & Li, Y. *Investigating the urban heat and cool islands during heatwaves in high density cities: A case study of Hong Kong from 2000-2018*.

Rohat, G., Flacke, J., Dosio, A., Pedde, S., Dao, H., & van Maarseveen, M. (2019). Influence of changes in socioeconomic and climatic conditions on future heat-related health challenges in Europe. *Global and Planetary Change*, *172*, 45-59. doi:10.1016/j.gloplacha.2018.09.013

Romero-Lankao, P., Qin, H., & Dickinson, K. (2012). Urban vulnerability to temperature-related hazards: A meta-analysis and meta-knowledge approach. *Global Environmental Change*, *22*(3), 670-683. doi:10.1016/j.gloenvcha.2012.04.002

Rosenthal, J. K., Kinney, P. L., & Metzger, K. B. (2014). Intra-urban vulnerability to heat-related mortality in New York City, 1997-2006. *Health & Place*, *30*, 45-60. doi:10.1016/j.healthplace.2014.07.014

Santamouris, M., & Kolokotsa, D. (2015). On the impact of urban overheating and extreme climatic conditions on housing, energy, comfort and environmental quality of vulnerable population in Europe. *Energy and Buildings*, *98*, 125-133.

Semenza, J. C., Rubin, C. H., Falter, K. H., Selanikio, J. D., Flanders, W. D., Howe, H. L., & Wilhelm, J. L. (1996). Heat-related deaths during the July 1995 heat wave in Chicago. *New England Journal of Medicine*, *335*(2), 84-90.

Shi, Y., Katzschner, L., & Ng, E. (2018). Modelling the fine-scale spatiotemporal pattern of urban heat island effect using land use regression approach in a megacity. *Science of the Total Environment, 618*, 891-904. doi:10.1016/j.scitotenv.2017.08.252

Shi, Y., Ren, C., Cai, M., Lau, K. K., Lee, T. C., & Wong, W. K. (2019). Assessing spatial variability of extreme hot weather conditions in Hong Kong: A land use regression approach. *Environmental Research, 171*, 403-415. doi:10.1016/j.envres.2019.01.041

Sun, Y., Zhang, X., Zwiers, F. W., Song, L., Wan, H., Hu, T., . . . Ren, G. (2014). Rapid increase in the risk of extreme summer heat in Eastern China. *Nature Climate Change, 4*(12), 1082-1085. doi:10.1038/nclimate2410

Tomlinson, C. J., Chapman, L., Thornes, J. E., & Baker, C. J. (2011). Including the urban heat island in spatial heat health risk assessment strategies: a case study for Birmingham, UK. *International Journal of Health Geographics, 10*(1), 42.

Uejio, C. K., Wilhelmi, O. V., Golden, J. S., Mills, D. M., Gulino, S. P., & Samenow, J. P. (2011). Intra-urban societal vulnerability to extreme heat: the role of heat exposure and the built environment, socioeconomics, and neighborhood stability. *Health & Place, 17*(2), 498-507. doi:10.1016/j.healthplace.2010.12.005

Verdonck, M. L., Demuzere, M., Hooyberghs, H., Priem, F., & Van Coillie, F. (2019). Heat risk assessment for the Brussels capital region under different urban planning and greenhouse gas emission scenarios. *Journal of Environmental Management, 249*, 109210. doi:10.1016/j.jenvman.2019.06.111

Victor, C., Scambler, S., Bond, J., & Bowling, A. (2000). Being alone in later life: loneliness, social isolation and living alone. *Reviews in Clinical Gerontology, 10*(4), 407-417.

Wang, D., Lau, K. K., Ren, C., Goggins, W. B. I., Shi, Y., Ho, H. C., . . . Ng, E. (2019). The impact of extremely hot weather events on all-cause mortality in a highly urbanized and densely populated subtropical city: A 10-year time-series study (2006-2015). *Science of the Total Environment, 690*, 923-931. doi:10.1016/j.scitotenv.2019.07.039

Wang, W., Zhou, W., Ng, E. Y. Y., & Xu, Y. (2016). Urban heat islands in Hong Kong: statistical modeling and trend detection. *Natural Hazards, 83*(2), 885-907. doi:10.1007/s11069-016-2353-6

Wang, Y., Li, Y., Sabatino, S. D., Martilli, A., & Chan, P. W. (2018). Effects of anthropogenic heat due to air-conditioning systems on an extreme high temperature event in Hong Kong. *Environmental Research Letters, 13*(3), 034015. doi:10.1088/1748-9326/aaa848

Watts, N., Amann, M., Arnell, N., Ayeb-Karlsson, S., Belesova, K., Boykoff, M., . . . Montgomery, H. (2019). The 2019 report of The *Lancet* Countdown on health and climate change: ensuring that the health of a child born today is not defined by a changing climate. *The Lancet, 394*(10211), 1836-1878. doi:10.1016/S0140-6736(19)32596-6

Wolf, T., Chuang, W. C., & McGregor, G. (2015). On the science-policy bridge: Do spatial heat vulnerability assessment studies influence policy? *International Journal of Environmental Research and Public Health, 12*(10), 13321-13349. doi:10.3390/ijerph121013321

Wolf, T., & McGregor, G. (2013). The development of a heat wave vulnerability index for London, United Kingdom. *Weather and Climate Extremes, 1*, 59-68. doi:10.1016/j.wace.2013.07.004

Wong, M. S., Peng, F., Zou, B., Shi, W. Z., & Wilson, G. J. (2016). Spatially Analyzing the Inequity of the Hong Kong Urban Heat Island by Socio-Demographic Characteristics. *International Journal of Environmental Research and Public Health, 13*(3). doi:10.3390/ijerph13030317

Wong, P. P.-Y., Lai, P.-C., Low, C.-T., Chen, S., & Hart, M. (2016). The impact of environmental and human factors on urban heat and microclimate variability. *Building and Environment, 95*, 199-208.

Wu, X. (2009). Income Inequality and Distributive Justice: A Comparative Analysis of Mainland China and Hong Kong. *The China Quarterly, 200*, 1033-1052. doi:10.1017/S0305741009990610

Zhang, W., Zheng, C., & Chen, F. (2019). Mapping heat-related health risks of elderly citizens in mountainous area: A case study of Chongqing, China. *Science of the Total Environment, 663*, 852-866. doi:10.1016/j.scitotenv.2019.01.240

Zhang, X., Ren, C., Lau, K., Shi, Y., Wang, D., & Ho, D. (2019). Towards a comprehensive heat-health warning system of Hong Kong: an evidence-based multi-stage approach. *Environmental Epidemiology, 3*, 463. doi:10.1097/01.Ee9.0000611232.71394.02

Spatiotemporal assessment of extreme heat risk for high-density cities: A case study of Hong Kong from 2006 to 2016

Supplementary Material

The values of VHDHs, HNHs, population density, and two vulnerability principal components for LTPUs were classified into five levels in order to uncover the underlying determinants behind the high-risk spots. The five categories are defined as:

1. Low: > 1.5 standard deviation (SD) below the mean,
2. Moderately low: 0.5–1.5 SD below the mean,
3. Moderate: 0.5 SD around the mean,
4. Moderately high: 0.5–1.5 SD above the mean,
5. High: > 1.5 SD above the mean.

The results are shown in Table 1.

Supplementary Table 1 Levels of heat hazard, exposure and vulnerability of the high-risk spots at the community level in Hong Kong

LTPU	Location	Area	VHDHs	HNHs	Population density	Elderly/Low-education/ Low-income/PRH	Living alone/ Low-quality housing
Daytime high-risk spots							
225	Yau Ma Tei	Kowloon	3	4	5	3	4
228	Yau Ma Tei	Kowloon	3	5	5	3	4
229	Mong Kok	Kowloon	3	5	5	4	4
266	Sham Shui Po	Kowloon	3	4	5	4	4
267	Sham Shui Po	Kowloon	3	4	5	3	4
287	Choi Hung	Kowloon	5	4	5	5	2
755	Sha Tin	New Territory	5	3	3	5	3
Nighttime high-risk spots							
113–114	Central and West	Hong Kong Island	3	5	3	3	5
116	Central and West	Hong Kong Island	2	4	5	4	4
132	Wan Chai	Hong Kong Island	3	5	3	3	5
225	Yau Ma Tei	Kowloon	3	5	5	3	4
228	Yau Ma Tei	Kowloon	2	5	4	3	4
221	Mong Kok	Kowloon	3	5	5	4	4
227	Mong Kok	Kowloon	3	4	5	3	4
229	Mong Kok	Kowloon	3	5	5	3	4
265	Sham Shui Po	Kowloon	3	4	5	3	3
266	Sham Shui Po	Kowloon	3	4	5	3	3
267	Sham Shui Po	Kowloon	3	4	5	4	4
241	To Kwa Wan	Kowloon	3	4	4	5	3
242	To Kwa Wan	Kowloon	3	4	5	4	4
243	To Kwa Wan	Kowloon	3	4	5	3	4
283	Wong Tai Sin	Kowloon	3	4	4	5	3
287	Choi Hung	Kowloon	5	4	5	5	2